

Non-Ideal Compressible Fluid Dynamics: A Challenge for Theory.

A. Kluwick¹

¹Institute of Fluid Mechanics and Heat Transfer, Technical University Vienna.

E-mail: alfred.kluwick@tuwien.ac.at

Abstract.

The possibility that compression as well as rarefaction shocks may form in single phase vapours was envisaged first by Bethe (1942). However calculations based on the Van der Waals equation of state indicated that the latter type of shock is possible only if the specific heat at constant volume c_v divided by the universal gas constant R is larger than about 17.5 which he considered too large to be satisfied by real fluids. This conclusion was contested by Thompson (1971) who showed that the type of shock capable of forming in arbitrary fluids is determined by the sign of the thermodynamic quantity

$$\Gamma = \frac{v^3}{2c^2} \frac{\partial^2 p}{\partial v^2} \bigg|_s$$

to which he referred to as fundamental derivative of gas dynamics. Here v , p , s and c denote the specific volume, the pressure, the entropy and the speed of sound. Thompson and co-workers also showed that the required condition for the existence of rarefaction shocks, that Γ may take on negative values, is indeed satisfied for a number of hydrocarbon and fluorocarbon vapours. This finding spawned a burst of theoretical studies elaborating on the unusual and often counterintuitive behaviour of shocks with rarefaction shocks present. These produced both results of theoretical character but also results suggesting the practical importance of Non-Ideal Compressible Fluid Dynamics in general. The present paper addresses some of the challenges encountered in connection with the theoretical treatment of the associated flow behaviour. Weakly nonlinear acoustic waves of finite amplitude serve as a starting point. Here mixed rather than strictly positive nonlinearity generates a wealth of phenomena not possible in perfect gases. Examples of steady flows where these non-classical effects play a decisive role (and which may be useful also for future experimental work) are quasi one-dimensional nozzle flows and transonic two-dimensional flows past corners. The study of viscous effects concentrates on laminar flows of boundary layer type. Here non-classical phenomena are caused by the uncommon smallness of the Eckert number but also by the unconventional Mach number dependence on p in the external inviscid flow region.

1. Introduction and Motivation

In 1983 I spent half a year at the Virginia Polytechnic Institute and State University in Blacksburg Va. One day Mark Cramer stepped into my office, handed me a paper



by Ph. Thompson entitled “A fundamental derivative in gas dynamics” and asked me to let him know my opinion. In this paper Thompson discusses the crucial effect of the curvature of isentropes in the pressure specific volume diagram for the dynamical behaviour of compressible fluids. Most conveniently this curvature is expressed in non-dimensional form

$$\Gamma = \frac{v^3}{2c^2} \frac{\partial^2 p}{\partial v^2} \Big|_s$$

where p, v, s and c denote the pressure, specific volume, specific entropy and sound speed. The symbol Γ is the one used by Hayes (1954) [13] but the notion fundamental derivative of gas dynamics had been coined by Thompson to emphasis its importance and in particular the importance of its sign in most areas of gas dynamics. The role the second derivative of p with respect to v at constant s plays in the theory of shock waves was however recognised much earlier. Concentrating on weak shocks in arbitrary gases Duhem (1909) [8] demonstrated that the entropy jump across such shocks is proportional to a quantity $H(p_1, v_1)$ and the third power of the jump of the specific volume:

$$[s] = -\frac{1}{12T_1 v_1^3} H(p_1, v_1) [v]^3. \quad (1)$$

Here p_1, v_1, T_1 denote the values of p, v and the absolute temperature T immediately upstream of the shock. Referring to the second law of thermodynamics Duhem thus concludes that shocks are of compressive/expansive type if $H > 0 / < 0$. It is easily shown that $H(p, v)$ can be written also in the form

$$H(p, v) = v^3 \frac{\partial^2 p}{\partial v^2} \Big|_s \quad (2)$$

and Duhem’s finding thus is equivalent to the statement that shocks are of compressive/expansive type if $\partial^2 p / \partial v^2|_s$ is $> 0 / < 0$ first formulated by Bethe (1942) [2] who apparently was unaware of Duhem’s work. An important further step towards the understanding of shocks in arbitrary fluids was taken by Becker (1922) [1] who, in his widely unknown Habilitationsschrift, showed that compression/expansion waves steepen if the curvature of isentropes is positive/negative and equally important that the resulting shocks automatically satisfy the second law of thermodynamics. Bethe’s lasting contribution to the theory of shocks is due to the fact that he did not stop when he reached his conclusion but - as also did the Russian scientist Zel’dovich (1946) [30] - went on to search for fluids having regions of negative isentropic curvature in the p, v diagram. Specifically he showed that van der Waals gases exhibit such regions in the general neighbourhood of the thermodynamic critical point if the ratio of the specific heat at constant volume c_v and the universal gas constant R is larger than about 17.5

$$\beta = \frac{c_v}{R} \gtrsim 17.5 \quad (3)$$

which he immediately dismissed as being physically impossible. Despite this negative statement Thompson (1971) [28] continued to investigate the dynamical behaviour of

such fluids and concludes that “for fluids with $\Gamma < 0$ the classical results of ordinary gas dynamics will be inverted”. As an example Fig.1 taken from the original publication shows the time evolution of a pressure pulse of triangular shape.

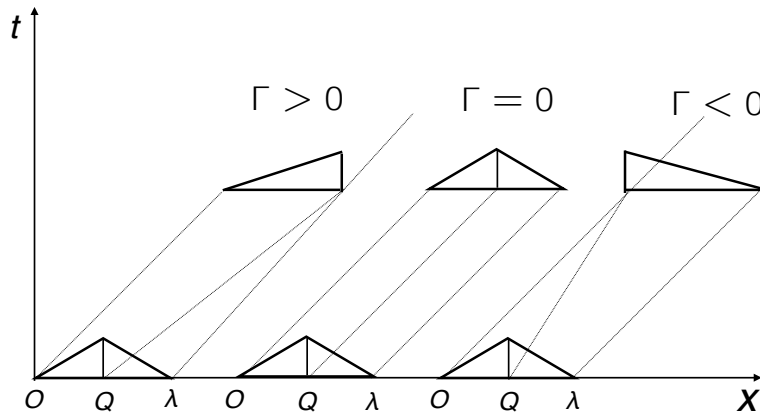


Figure 1. Time evolution of pressure pulse in the space (x) - time (t) diagram.

As pointed out before, compression waves steepen while rarefaction waves spread out if $\Gamma > 0$. In contrast, rarefaction waves steepen while compression wave spread out if $\Gamma < 0$. Therefore only compression shocks will form in a positive Γ fluid and only rarefaction shocks will form in a negative Γ fluid. Thompson then concluded: “the existence of rarefaction shocks is consistent with the tendency of rarefaction waves to steepen. Thus, if certain results are inverted, others necessarily follow. The interest in such phenomena is quite academic, however, if no real fluids with negative Γ exist. We believe that such fluids exist and will report specifically in the near future.” Indeed theoretical evidence for the existence of such fluids was provided already in 1972 by Lambrakis and Thompson [23] and in more detail in 1973 by Thompson and Lambrakis [28]. In 1983 the list of negative Γ fluids included several dense gases such as hydrocarbons and fluorocarbons of practical interest. So, when Mark Cramer entered my office several days later I told him that I was interested in joint research in this area provided we concentrated on aspects of fluid mechanics rather than the search for further candidates of negative Γ fluids as in my opinion the existing literature formed a sufficiently strong and reliable basis for such efforts. This is supported also by more recent investigations by Colonna, Guardone and Nannan (2007) [3] which point to the existence of a new class of negative Γ fluids so-called Siloxanes. This then sets the stage for this paper which will be based on the premise that negative Γ fluids exist and will concentrate on the associated aspects of non-ideal compressible fluid dynamics.

2. Theoretical building blocks

2.1. Shock formation

As a starting point we go back to the problem of acoustic wave propagation and treat the formation of shocks in simple right running waves in more detail.

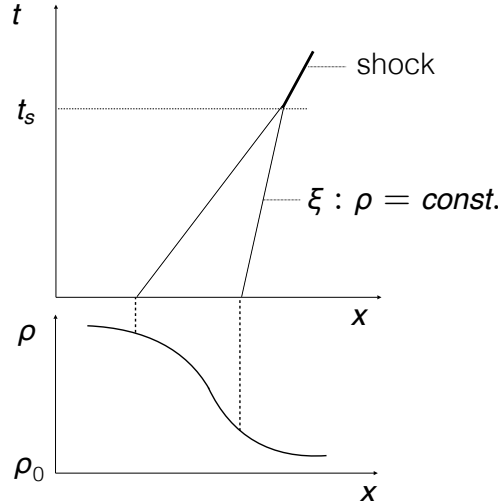


Figure 2. Shock formation by intersecting characteristics $\xi(x, t) = \text{const.}$

As sketched in Fig.2 we assume that the density distribution imposed at the initial time is a smooth function of the propagation distance x and as in classical gas-dynamics the density ρ is constant on wave fronts or characteristics $\xi(x, t) = \text{const.}$ propagating with speed v_w which depends on ρ only, Fig. 2. Making use of the relationship

$$\frac{dv_w}{d\rho} = \frac{c}{\rho}\Gamma \quad (4)$$

first derived by Becker (1922) [1] it is easily shown that neighbouring characteristics intersect at times $t = \frac{\rho}{c\Gamma} \frac{d\rho}{d\xi}$ and the minimum value defines the shock formation time:

$$t_s = \min\left(\frac{\rho}{c\Gamma} \frac{d\rho}{d\xi}\right). \quad (5)$$

If the fundamental derivative Γ is of $O(1)$ as in the case of dilute, i.e. perfect gases and if the wave carries small density disturbances

$$\frac{\rho - \rho_0}{\rho_0} = O(\epsilon), \quad \epsilon \ll 1 \quad (6)$$

t_s is of $O(1/\epsilon)$ as known from classical acoustics. If, however, Γ is small t_s increases drastically and tends to infinity as Γ tends to zero. We thus conclude that non-linear effects in dense gases having small values of Γ - positive or negative - are significantly weaker than in classical gases leading in turn to a delay of shock formation.

2.2. Wave evolution

Following the discussion of shock formation we next consider the evolution of the wave profile as a whole. To this end we express the requirement that ρ is constant on characteristics propagating with speed v_w as

$$\frac{\partial \rho}{\partial t} + v_w \frac{\partial \rho}{\partial x} = 0. \quad (7)$$

Further simplification is achieved by introducing the quantity $j(\rho)$:

$$\frac{dj}{d\rho} = v_w(\rho). \quad (8)$$

The wave evolution then is governed by the equation

$$\frac{\partial \rho}{\partial t} + \frac{\partial j(\rho)}{\partial x} = 0 \quad (9)$$

which has the form of a continuity equation. The physical meaning of $j(\rho)$ thus is obvious: it represents the perturbation mass flux carried by the wave. The equation for j has to be solved numerically in general. However analytical progress is possible if the density disturbances caused by the wave are small, Cramer and Kluwick (1984) [4], Kluwick (1991) [17]. Equally important $j(\rho)$ then has universal meaning, i.e., is of relevance not only for acoustic waves but also for most areas of gas dynamics.

2.3. Shock propagation

To complete the theoretical basis for the treatment of dense gas flows it is finally necessary to consider the process of shock propagation. Assuming one-dimensional steady flow as in Fig. 3 where w, p, v and h denote the flow velocity in the x direction, the pressure, the specific volume and the specific enthalpy. Subscripts 1 and 2 specify values immediately upstream and downstream of the shock while square brackets denote the jump of any physical quantity, say q : $[q] = q_2 - q_1$.

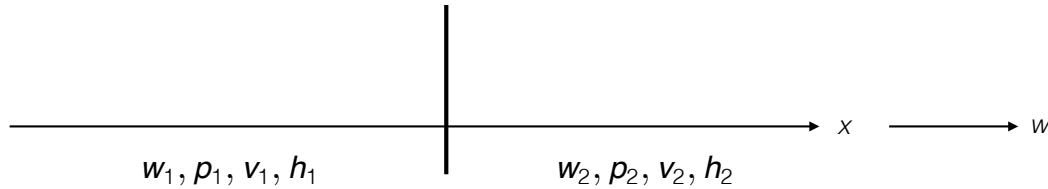


Figure 3. Shock propagation.

The balances of mass, momentum and energy in integral form then yield the celebrated Rankine-Hugoniot relationship

$$[h] = [p](v_1 + v_2)/2 \quad (10)$$

which contains thermodynamic quantities only and therefore holds for arbitrary fluids. Specific fluid properties enter via the caloric equation of state

$$h = h(p, v) \quad (11)$$

and when combined with the Rankine - Hugoniot relationship yields the shock adiabat

$$p_2 = f(p_1, v_1; v_2). \quad (12)$$

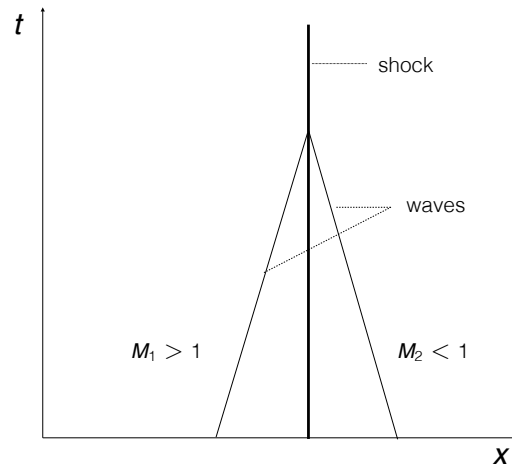


Figure 4. Wave speed ordering relationship

If one specifies values p_1, v_1 upstream of the shock and v_2 downstream the formal solution of the shock adiabat predicts the downstream value of the pressure p_2 . But the question then arises: are all formal solutions also physically realisable? This is the so called admissibility problem. Of course, a necessary requirement is provided by the second law of thermodynamics which states that the specific entropy must not decrease during adiabatic changes of state. A second natural requirement is that shocks must be able to form mechanically through intersecting characteristics, Fig. 4. Therefore, the Mach number $M = w/c$ has to be larger than one upstream and smaller than one downstream of the shock which sometimes is summarised as the wave speed ordering relationship: $M_1 > 1 > M_2$.

As pointed out before, Thompson and his doctoral student Lambrakis, making use of more sophisticated equations of state than the van der Waals equation of state considered by Bethe, were the first to demonstrate the existence of real negative Γ fluids and thus also the possible existence of single phase rarefaction shocks. Honouring the pioneering work of Bethe, Zel'dovich and Thompson such fluids are now commonly termed Bethe-Zel'dovich-Thompson fluids or in short BZT fluids. Interestingly, the existence of such fluids is suggested already by pure theoretical reasoning independent of any assumptions concerning specific forms of equations of state, namely by taking

into account that the specific internal energy $u(v, T)$ and the specific entropy $s(v, T)$ can be decomposed in this form:

$$u(v, T) = \phi(T) + \beta^{-1}f(v, T), \quad s(v, T) = \psi(T) + \beta^{-1}g(v, T). \quad (13)$$

Here $\phi(T)$ and $\psi(T)$ depend on the ideal gas heat capacity $c_{v\infty}$, i.e. the limiting value of c_v as v tends to infinity only and β is the parameter introduced by Bethe (1942) [2] which measures the relative magnitude of $c_{v\infty}$ evaluated at the critical point temperature and the universal gas constant R . For perfect gases and other gases of low molecular complexity β is of $O(1)$ and the dependence of u and s on v and T is equally important. However, for gases of moderate and high molecular complexity β is large and both quantities depend mainly on T with small corrections of $O(1/\beta)$ due to variations of v accounted for by the functions $f(v, T)$ and $g(v, T)$. Substitution of expressions (13) into the Rankine-Hugoniot relationship assuming β to be large then yields the result that temperature changes caused by shocks are small and of $O(1/\beta)$:

$$\frac{[T]}{T_1} = O(\beta^{-1}). \quad (14)$$

As a consequence, shock adiabats, isotherms and isentropes differ little in the p, v diagram. Therefore, in the definition of the fundamental derivative Γ derivatives at constant s can be approximated by derivatives at constant T

$$\Gamma = \frac{v^3}{2c^2} \left(\frac{\partial^2 p}{\partial v^2} \right)_s = \frac{v^3}{2c^2} \left(\frac{\partial^2 p}{\partial v^2} \right)_T + O(\beta^{-1}) \quad (15)$$

and since isotherms are known to have negative curvature in the general neighbourhood of the thermodynamic critical point it is expected that Γ will be negative there also.

As pointed out before β is large for gases with large specific heats and, therefore, such gases are candidates of BZT fluids. As an example Fig.5 displays results for van der Waals gases having values $1/\beta$ equal to 0.02 and 0.001. p and v are non-dimensional with their critical point values p_c and v_c . In both cases there exists a region of negative Γ bounded by the so called transition line $\Gamma = 0$. While for $1/\beta = 0.02$ the difference between shock adiabats, isotherms and isentropes is still clearly visible they almost collapse for the smaller value $1/\beta = 0.001$. For the treatment of shocks in BZT fluids it is essential to acknowledge the qualitative changes of the shock adiabat associated with increasing values of β , Fig.6. If β is of $O(1)$ shock adiabats are curved upwards as in the case of perfect gases. For large values of β , however, shock adiabats exhibit two inflexion points separated by a bulge with negative curvature.

To simplify the analysis we make use of the relationship

$$\frac{[p]}{[v]} = -\rho_1^2 w_1^2 = -\rho_2^2 w_2^2 \quad (16)$$

which relates the slope of the straight line, the so called Rayleigh line, which connects the upstream and downstream states on the shock adiabat with the square of the associated mass flux, Fig.7.

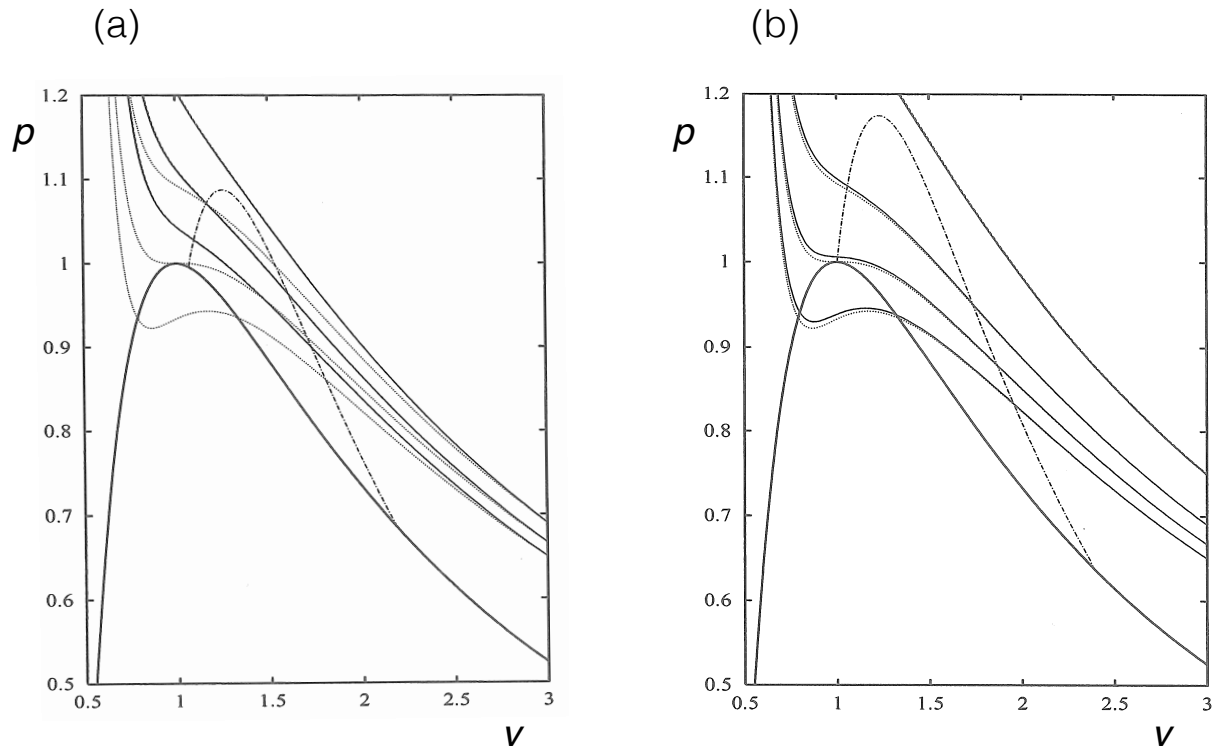


Figure 5. — Isentropes, ---- shock adiabats and isotherms for van der Waals gases with (a) $1/\beta = 0.02$ and (b) $1/\beta = 0.001$. — saturation line, ---- $\Gamma = 0$ locus.

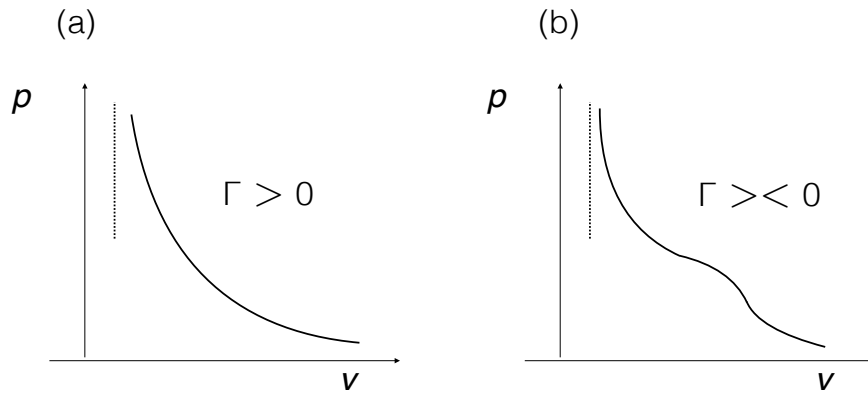


Figure 6. Qualitative shape of shock adiabats for (a) $\beta = O(1)$ and (b) $\beta \gg 1$.

For the following, two properties of the Rayleigh line are of importance, see e.g. Kluwick (2001) [21]. First, it can be shown that the wave speed ordering relationship is satisfied if the Rayleigh line does not cut the shock adiabat in interior points. Therefore, a shock with upstream and downstream pressures p_1, p_2 is admissible while a shock with

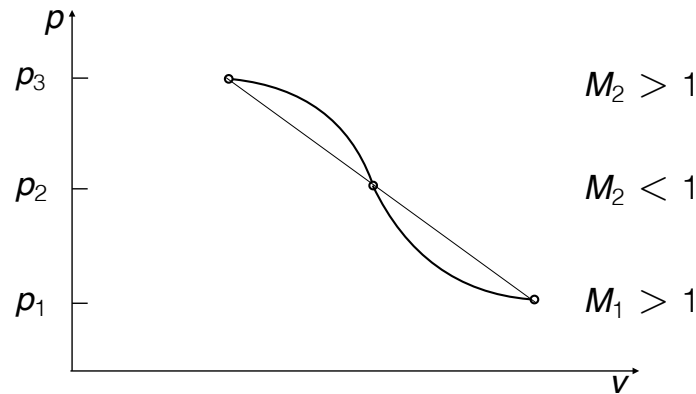


Figure 7. Admissible and inadmissible shocks. — shock adiabat, — Rayleigh line.

downstream pressure p_3 is inadmissible. Second, it can be shown that if the Rayleigh line is tangent to the shock adiabat in some point, Fig.8, then the Mach number M associated with this state is equal to one and the distribution of the specific entropy along the shock adiabat exhibits an extremum.

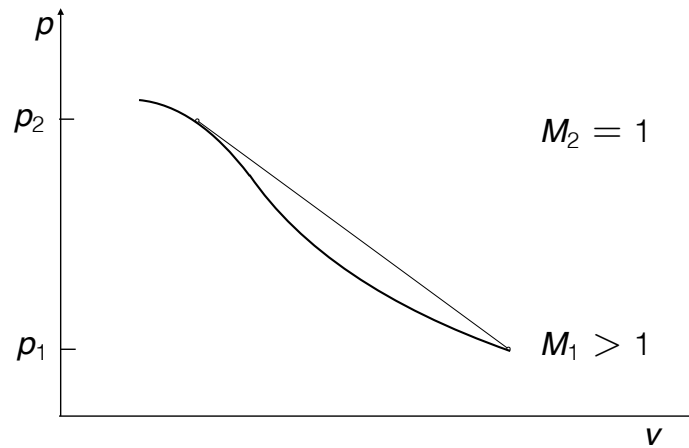


Figure 8. Shock with sonic downstream conditions. — shock adiabat, — Rayleigh line.

These results motivated Lax (1957) [24] and Oleinik (1959) [25] to propose the extended wave speed ordering relationship $M_1 \geq 1 \geq M_2$ which allows the existence of non-classical shocks with Mach number 1 upstream or downstream (sonic shocks) or even with Mach number 1 upstream and downstream (double sonic shocks). Representative examples are shown in Fig.9.

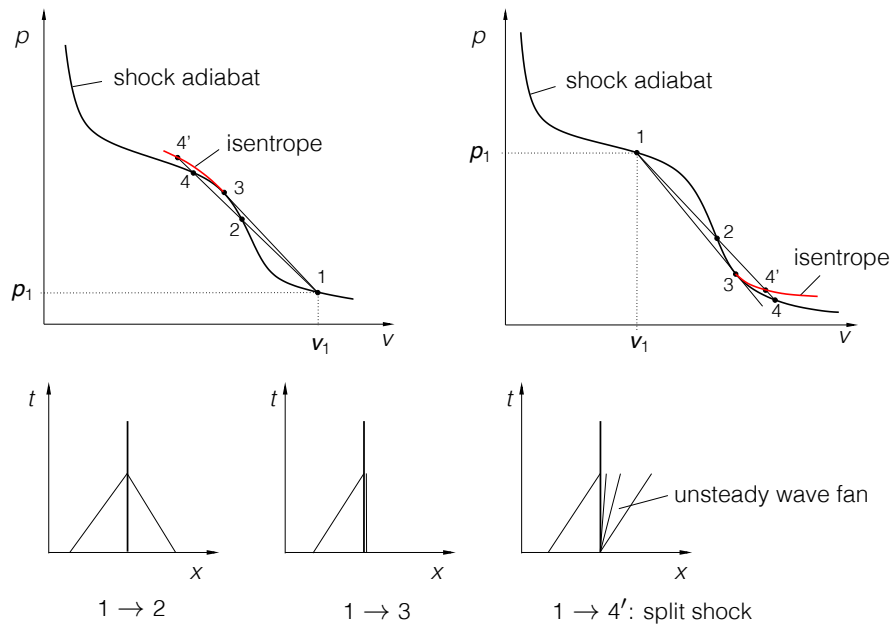


Figure 9. Admissible and inadmissible compression/rarefaction shocks

First let us consider compression shocks with an upstream state 1. Shocks leading to a downstream state 2 are clearly admissible as the associated Rayleigh line is located entirely above the shock adiabat so that the wave speed ordering relationship is satisfied as shown in the x, t diagram. By increasing the shock strength one approaches state 3 where the Rayleigh line is tangent to the shock adiabat indicating that a sonic downstream state has been reached: in the x, t diagram the shock front coincides with the wave front downstream of the shock. Also it is seen that single shocks of even higher strength, leading e.g. from state 1 to state 4 are inadmissible as the Rayleigh line then cuts the shock adiabat. By imposing a larger pressure increase we obtain the following structure: the shock from state 1 to state 3 with sonic downstream conditions is followed by a continuous compression of the fluid along the isentrope starting in point 3 which generates a compression wave fan in the space-time diagram and represents another non classical feature of BZT fluids. The resulting compound structure consisting of a sonic compression shock and an attached compression wave fan is termed a compression split shock.

The diagram on the right hand side of Fig.9 shows that the scenario resulting from the consideration of rarefaction shocks of variable strength is completely analogous to that obtained for compression shocks: by increasing the shock strength, i.e. by reducing the downstream pressure, a sonic downstream state 3 is reached eventually. Further decrease of the downstream pressure is possible only through a rarefaction split shock, i.e. through the combined action of a sonic rarefaction shock and an attached rarefaction wave fan.

3. Weakly nonlinear progressive waves

The results summarised in Section 2 provide the building blocks necessary to treat specific problems e.g. acoustic waves which served as the starting point of our considerations. To simplify these considerations we concentrate on waves which carry small density disturbances

$$\frac{\rho - \rho_0}{\rho_0} = \epsilon \rho_1 + O(\epsilon^2), \quad \epsilon \ll 1. \quad (17)$$

Such an approach yields a complete qualitative picture of all possible phenomena and allows for significant analytical progress. Taylor expansion of the perturbation mass flux $j(\rho)$ involves the values Γ_0, Λ_0, N_0 of the fundamental derivative and its first and second derivative with respect to ρ evaluated in the unperturbed state. By introducing suitably scaled quantities

$$\bar{\rho}_1 = \frac{\Lambda_0}{\Gamma_0} \rho_1, \quad \bar{j}_1 = \frac{\Lambda_0^2}{\Gamma_0^3} j_1, \quad (18)$$

one then obtains the remarkable result that the representation of \bar{j}_1 in terms of $\bar{\rho}_1$ depends on a single similarity parameter \hat{N}_0 only

$$\bar{j}_1 = \frac{1}{2} \bar{\rho}_1^2 + \frac{1}{6} \bar{\rho}_1^3 + \frac{\hat{N}_0}{12} \bar{\rho}_1^4, \quad \hat{N}_0 = \frac{N_0 \Gamma_0}{\Lambda_0}. \quad (19)$$

Graphs \bar{j}_1 versus $\bar{\rho}_1$ are depicted in Fig.10 for two values of \hat{N}_0 including $\hat{N}_0 = 0$.

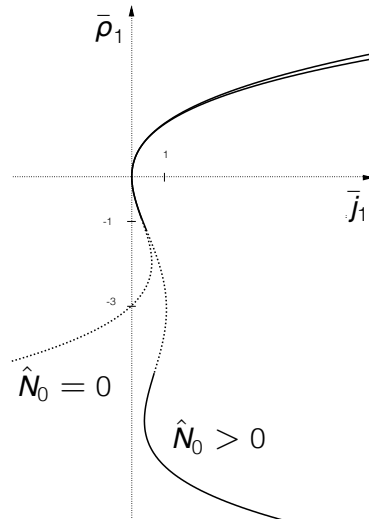


Figure 10. Representative examples of $\bar{j}_1, \bar{\rho}_1$ diagrams; — $\Gamma > 0$, $\Gamma < 0$.

By making use of the expression

$$\bar{\Gamma} = \frac{\Gamma}{\Gamma_0} = \epsilon^2 \frac{d^2 \bar{j}_1}{d \bar{\rho}_1^2} \quad (20)$$

we infer that inflexion points in Fig.10 separate regions of positive Γ (solid lines) and regions of negative Γ (dotted lines). As a representative example of progressive waves generated by localised disturbances we investigate the evolution of square pulses specified by initial conditions at $\tau = \epsilon^3 c_0 t / L = 0$, Fig. 11.

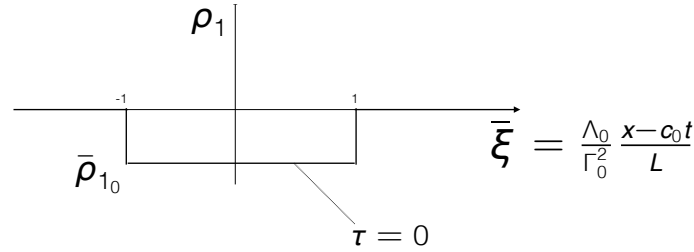


Figure 11. square pulse

Here $\bar{\rho}_1$ vanishes for values of the transformed propagation distance $\bar{\xi} > 1$, $\bar{\xi} < -1$ and assumes the constant value $\bar{\rho}_{1_0}$ in between. For $\bar{\rho}_{1_0} > -1$ the fluid remains in the positive Γ region and, consequently, the wave evolution is qualitatively similar to the predictions of classical nonlinear acoustics: a rarefaction wave fan forms at $\bar{\xi} = 1$, the pulse is terminated by a compression shock and the wave profile eventually approaches a linear density distribution as τ tends to infinity, Fig.12.

For $\bar{\rho}_{1_0} = -2.2$ the density disturbances inside the pulse are large enough for Γ to change sign which is seen to lead to significant changes of the wave pattern, Fig.13. Specifically it is found that a rarefaction wave fan at $\bar{\xi} = 1$ taking the fluid from the unperturbed to the perturbed state is no longer possible but requires the combined action of a sonic rarefaction shock and an attached rarefaction wave fan. Also the discontinuous increase of $\bar{\rho}_1$ at the wave tail no longer generates a single compression shock but results in the formation of a compression wave fan and a sonic compression shock. Both shock-fan combinations are weakly nonlinear versions of finite amplitude split shocks described in section 2.3. The sonic rarefaction shock is weakened by its interaction with the compression wave fan. It emanates characteristics in the tangential direction thereby generating a so-called precursor region. This has the distinguishing feature that the characteristics are no longer connected with the initial data but that information propagates along characteristics that cross the sonic rarefaction shock. Another interesting phenomenon arises from the collision of the sonic rarefaction and compression shocks at $\tau = \tau_c$. While according to the classical theory of weakly nonlinear acoustics two merging shocks result in a single shock of larger amplitude, the collision of a rarefaction and a compression shock is seen to be associated with the formation of a sharp spike in the density distribution as τ approaches τ_c and a sudden reduction of the shock strength at $\tau = \tau_c$.

We conclude the discussion of weakly nonlinear progressive waves by considering a square pulse of even larger negative amplitude, large enough to take the fluid across the whole negative Γ region. The resulting wave pattern then exhibits an astounding

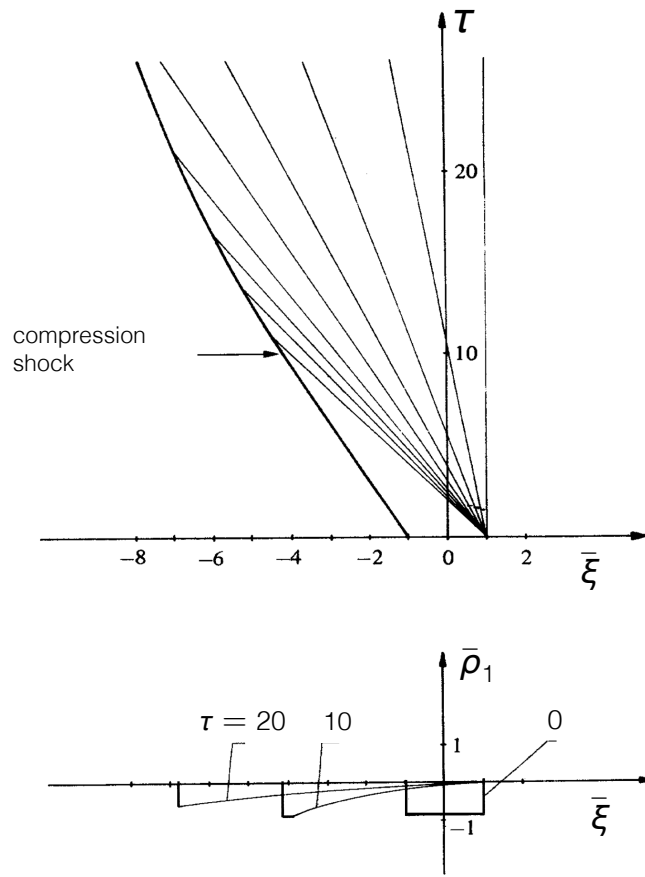


Figure 12. evolution of square pulse: $\hat{N}_0 = 0, \bar{\rho}_{1_0} = -0.9$

richness of wave fans, sonic shocks and double sonic shocks, Fig.14. The three examples of weakly nonlinear acoustic waves may be of limited value as far as practical applications are concerned. However, they demonstrate how the complexity of dense gas flows increases dramatically if non classical phenomena such as compression wave fans, sonic shocks and double sonic shocks come into play. Clearly, two and three dimensional unsteady flows are expected to exhibit even more complex behaviour which in part explains the difficulty to perform clean shock tube experiments where three dimensional disturbances can hardly be avoided. In the following we shall, therefore, concentrate on steady flows through Laval nozzles and two dimensional external flows which are of interest on their own and where unwanted disturbances may be controlled more easily in experimental work.

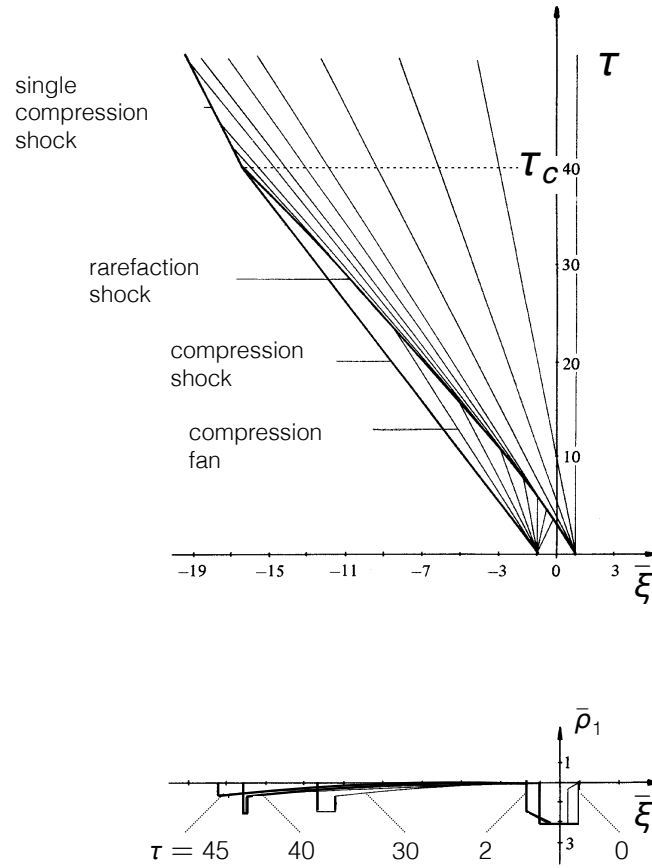


Figure 13. evolution of square pulse: $\hat{N}_0 = 0, \bar{\rho}_{10} = -2.2$

4. Weakly nonlinear steady flow

4.1. Flow through slender nozzles

Transonic quasi - one dimensional flow through slender nozzles, Fig.15, is governed by the equation

$$\frac{\partial \rho_1}{\partial \tau} + \frac{1}{2} \frac{\partial j_1}{\partial x} = -\frac{1}{2} \frac{dA_1}{dx} \quad (21)$$

where unsteady effects are included for the moment, Kluwick (1993) [18], Kluwick and St.Scheichl (1996) [19]. A_1 characterises the variation of the area of cross section relative to its value A_0 at the throat

$$\frac{A}{A_0} = 1 + \epsilon^4 A_1. \quad (22)$$

As before ϵ is a small perturbation parameter and that it enters the analysis at $O(\epsilon^4)$ reflects the extreme sensitivity of transonic flows with respect to changes of stream tube area. In the case of steady flow (21) can immediately be integrated to yield

$$j_1 + A_1 = Q \quad (23)$$

where Q is an integration constant. It is convenient to require $\rho_1 = 0$ if the local Mach number M equals 1 which leads to the following representation for the perturbation

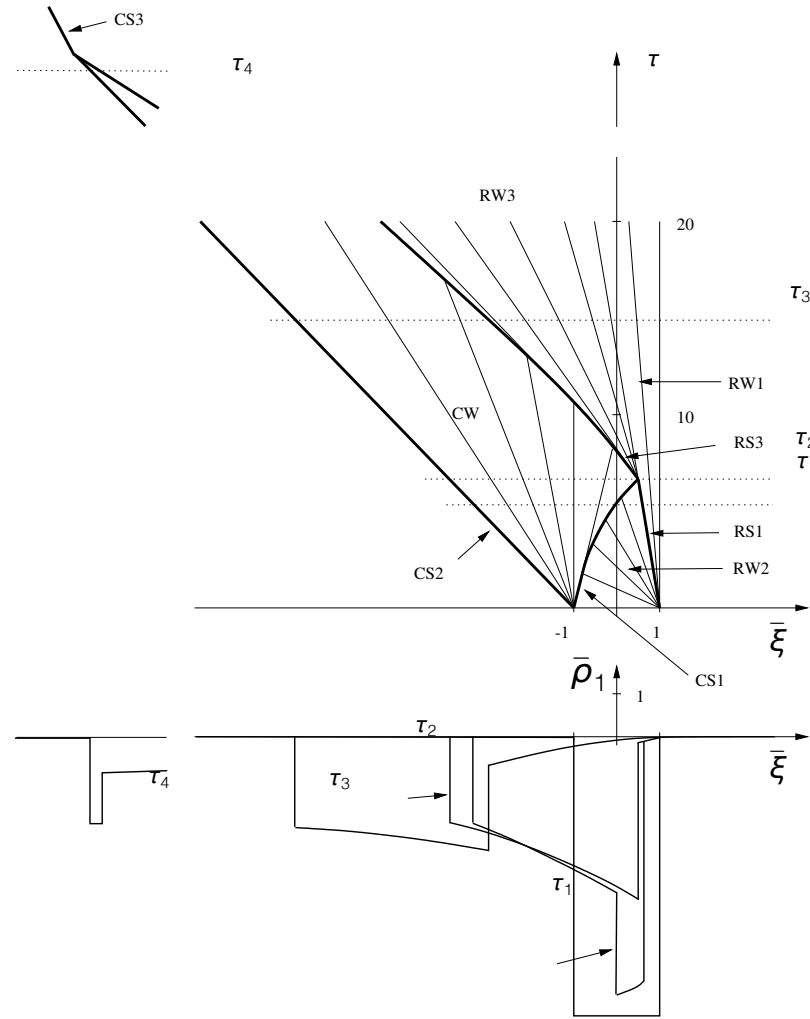


Figure 14. evolution of square pulse: $\hat{N}_0 = 0.342$, $\bar{\rho}_{10} = -6.5$

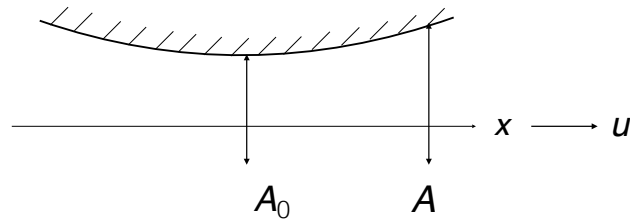


Figure 15. transonic slender nozzle flow

mass flux j_1 obtained by a Taylor series expansion:

$$j_1 = -\hat{\Gamma}_0 \rho_1^2 - \frac{1}{3} \hat{\Lambda}_0 \rho_1^3 - \frac{1}{12} \hat{N}_0 \rho_1^4. \quad (24)$$

j_1 includes constants which are suitably scaled values of the fundamental derivative Γ and its first and second derivative with respect to the fluid density in the unperturbed state. We note that the above perturbation approach has recently been generalised in Vimercati (2015) [29], Guardone and Vimercati (2016) [12] where, as in the numerical study by Cramer and Fry (1993) [6], the exact expression for the perturbation mass flux is taken into account rather than its approximation by equation (24). As a first specific example we consider convergent-divergent Laval nozzles such that A_1 is a quadratic function of the distance x measured from the throat: $A_1 = Cx^2$. If $\hat{\Gamma}_0$ satisfies the inequality

$$\hat{\Gamma}_0 > \frac{3\hat{\Lambda}_0^2}{8\hat{N}_0} \quad (25)$$

the flow is of classical type where Γ is positive throughout and a sonic state is reached only once. Solutions form two branches of continuously accelerating or decelerating flows leading, respectively, from subsonic to supersonic or from supersonic to subsonic conditions. In addition, there exist flows with compression shocks present in the diverging part of the nozzle, Fig.16.

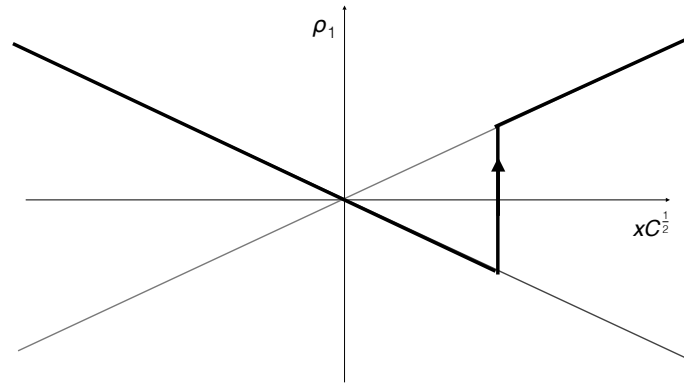


Figure 16. Laval nozzle: possible density distributions. $\hat{\Gamma}_0 = 24.06$, $\hat{\Lambda}_0 = 30.96$, $\hat{N}_0 = 19.22$.

Fig.17 shows how these conventional flow patterns change if $\hat{\Gamma}_0$ is reduced so that the flow then takes the fluid across the whole negative Γ region and there exist three sonic states rather than a single one, Kluwick(1993) [18]. It is seen that density distributions are no longer single-valued but exhibit regions of multi-valuedness which have to be eliminated by the insertion of shock discontinuities. Consequently, shock free flow is not possible but instead we observe flow configurations with one, two or even three shocks present. This naturally raises the question: can dense gases of BZT type be accelerated shock free from subsonic to supersonic speeds? To answer this question we formulate

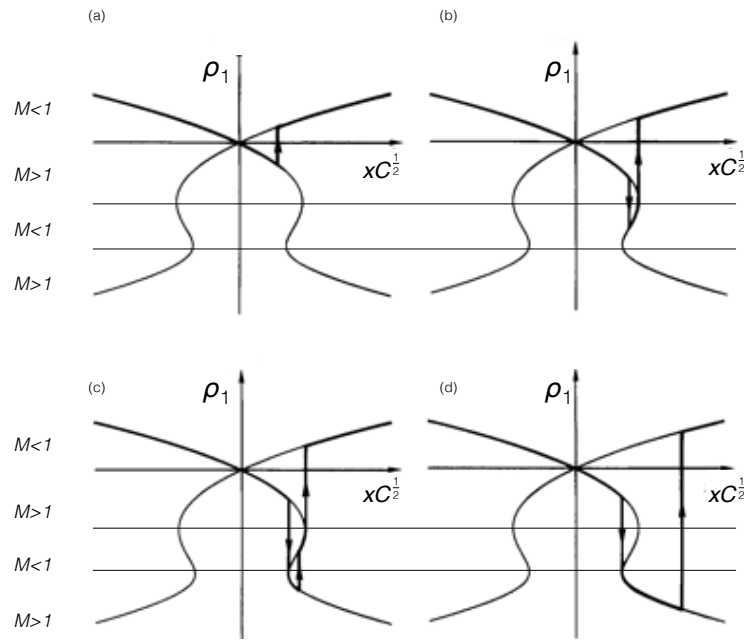


Figure 17. Laval nozzle: possible density distributions. $\hat{\Gamma}_0 = 4.91, \hat{\Lambda}_0 = 15.80, \hat{N}_0 = 17.67$.

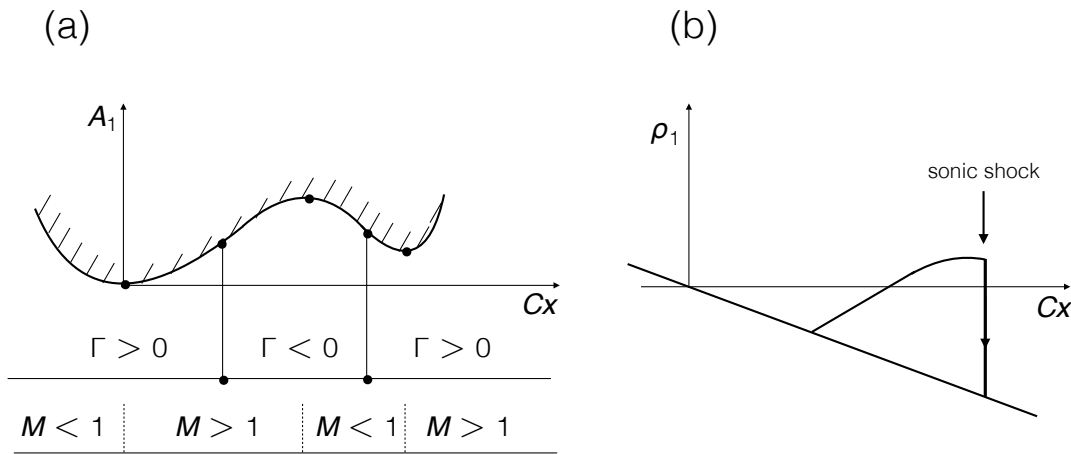


Figure 18. (a) Nozzle shape designed to generate a shock free transition from subsonic to supersonic flow conditions. (b) Associated density distributions. $\hat{\Gamma}_0 = 4.91, \hat{\Lambda}_0 = 15.80, \hat{N}_0 = 17.67$.

an inverse problem: we prescribe the desired density distribution, e.g. a linear one

$$\rho_1 = -Cx, \quad C > 0 \quad (26)$$

and use the continuity equation to determine the necessary nozzle shape. One then finds that a nozzle with two throats and an intervening anti-throat is required to achieve a

subsonic-supersonic transition from a state with positive Γ to another positive Γ state which passes through the whole negative Γ region, Fig.18 a. However, one also observes that in addition to the prescribed density distribution there exists a second solution branch which exhibits a sonic shock, Fig.18b. So which of these solutions will be realised in practice? To my knowledge a definite answer is not known at present but calculations carried out with the aim to understand how the steady state solution is reached by means of an unsteady starting process governed by the full equation (21) appear to favour the solution with the sonic shock present, Kluwick and Scheichl (1996) [19]. To obtain a definitive answer however will require an extension of the present theory beyond the first order approximation in order to account for the differences between the density and pressure disturbances due to entropy changes caused by shocks. Alternatively the theory developed in Guardone and Vimercati (2016) [12], Vimercati (2015) [29] might be used to clarify this point.

4.2. Two dimensional external transonic flow

As a last example of inviscid gasdynamics we consider transonic external flows, Cramer and Tarkenton (1992) [5]. Specifically we concentrate on two dimensional ramp configurations as sketched in Fig. 19.

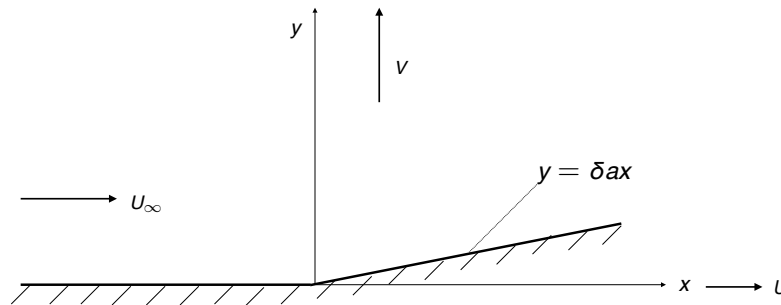


Figure 19. Transonic flow past compression/expansion ramps

Herein x, y and u, v denote Cartesian coordinates parallel and normal to the incoming flow and the corresponding velocity components. Parameters δ and a define the ramp angle. We assume that the ramp angle is small, i.e. we require that $a = O(1)$ while $\delta \ll 1$. The governing equations

$$\frac{\partial j}{\partial x} + \frac{\partial v}{\partial y} = 0, \quad \frac{\partial u}{\partial y} - \frac{\partial v}{\partial x} = 0, \quad j(u) = (1 - M_\infty^2)u - \Gamma_\infty u^2 + \frac{\Lambda_\infty}{3}u^3 \quad (27)$$

include the continuity equation and the requirement of irrotational flow. Five different

flow regimes characterised by two non-dimensional similarity parameters

$$K_1 = \frac{M_\infty^2 - 1}{(\delta\Gamma_\infty)^{\frac{2}{3}}}, \quad K_2 = \frac{\delta^{\frac{2}{3}}\Lambda_\infty}{\Gamma_\infty^{\frac{4}{3}}} \quad (28)$$

can be identified, Kluwick and Cox (2016) [22]. For upstream supersonic flow considered here only K_1 is strictly positive while K_2 can be positive or negative.

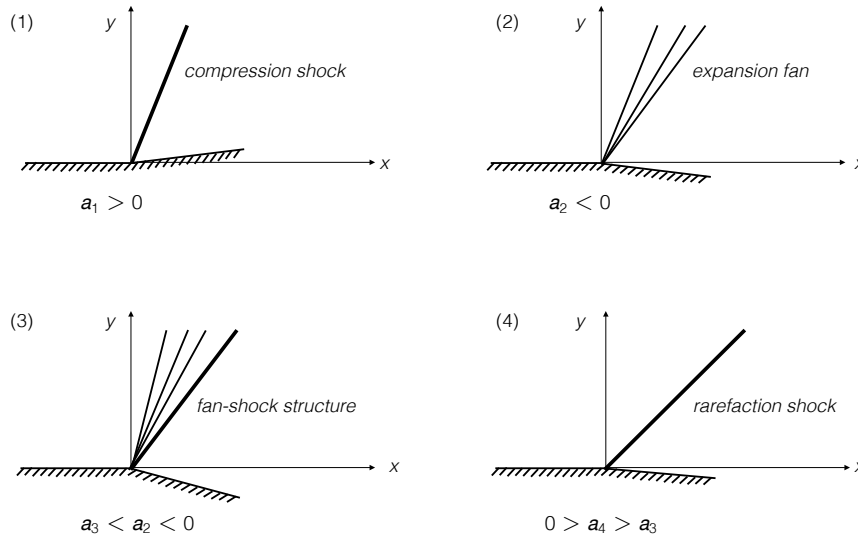


Figure 20. Possible wave patterns for $K_1 > 0, K_2 > 0$ fixed, $\Gamma_\infty > 0, a > < 0$

As a representative example Fig.20 displays results for $K_2 > 0$ and $\Gamma_\infty > 0$. For positive ramp angles $a > 0$ we observe a single compression shock while expansion ramps causing small negative turning angles $a < 0$ generate pure expansion fans in agreement with intuition based on classical gas dynamics. Non classical effects, however, arise if the negative ramp angle is increased which causes the emergence of a rarefaction shock with sonic upstream conditions. With ramp angle a decreasing even further the wave fan shrinks in size which finally results in the formation of a single rarefaction shock.

Fig.21 shows solutions of a different type of problem first posed by Guardone, Colonna, Casati and Rinaldi (2014) [11] where the ramp angle a is kept constant while the fluid properties upstream of the ramp vary. Specifically we consider an expansive ramp with $a = -1.6$ and assume $K_1 = 1$. As K_2 increases from -5.5 to 1.5 the flow pattern changes from a centred wave fan to a single shock in full qualitative agreement with the numerical results presented by Guardone et al. (2014) [11].

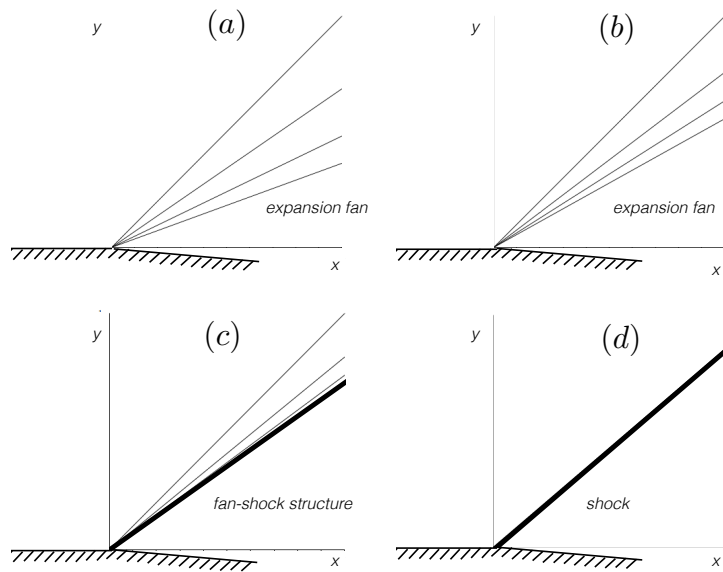


Figure 21. Possible wave patterns for $K_1 = 1, a = -1.6$ and K_2 varying between -5.5 and 1.5 .

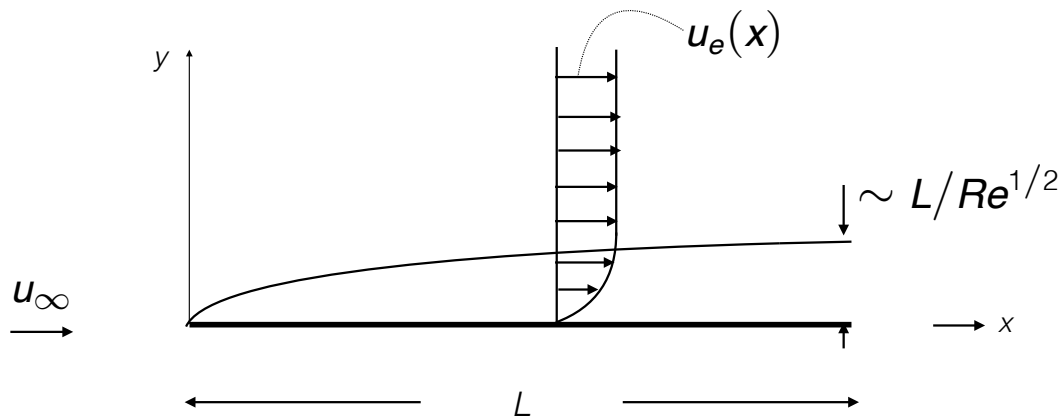


Figure 22. Laminar boundary layer on a flat plate

5. Laminar boundary layers

Following the outline of inviscid flows given in the preceding sections we now turn to a brief discussion of dissipative effects. To simplify this discussion I shall concentrate on laminar flows of boundary layer type. A representative example, see Fig.22, is given by the boundary layer which forms on a flat plate of length L in the limit of large Reynolds number.

$$Re = \frac{u_\infty L \rho_\infty}{\mu_\infty} \gg 1. \quad (29)$$

Here u , ρ and μ denote the velocity component parallel to the plate, the density and the dynamic viscosity. Subscripts ∞ and e refer to quantities evaluated under free stream conditions and at the boundary layer edge. If the Reynolds number is scaled out as usual the nondimensional groups which enter the boundary layer equations are the Prandtl number, the coefficient of thermal expansion α_∞ non dimensional with T_∞ and the Eckert number

$$Pr = \frac{\mu_\infty c_{p\infty}}{\lambda_\infty}, \quad \alpha_\infty T_\infty, \quad Ec = \frac{u_\infty^2}{c_{p\infty} T_\infty} \quad (30)$$

λ and c_p are, of course, the thermal conductivity and the specific heat at constant pressure. Similar to perfect gases the Prandtl number and $\alpha_\infty T_\infty$ are of $O(1)$ also for dense gases if the immediate neighbourhood of the thermodynamic critical point is excluded from the considerations. In contrast, however, the Eckert number no longer is of $O(M_\infty^2)$ but of $O(M_\infty^2/\beta)$. As pointed out before the quantity β introduced by Bethe increases with increasing molecular complexity and typical values for vapours of BZT fluids are in the range of 100 to 150. As a consequence dissipation caused by internal friction and heat conduction can be neglected even at moderately large supersonic Mach numbers. For flows past adiabatic walls this means that the temperature and thus also the fluid density is nearly constant across the boundary layer.

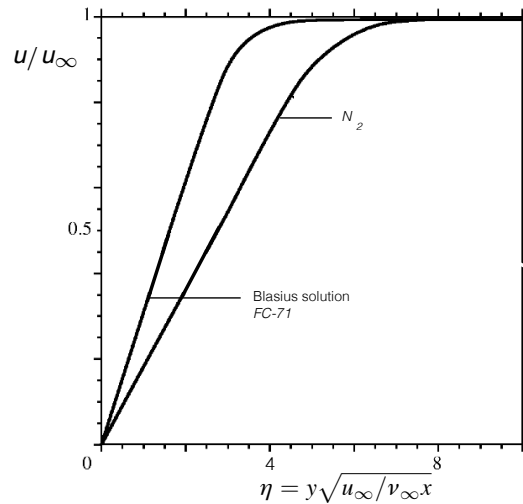


Figure 23. Flat plate boundary layers

As an example Fig.23 shows the velocity distribution across a flat plate boundary layer with zero pressure gradient at $M_\infty = 2$ for N_2 and the BZT fluid pf-trihexylamine ($C_{18}F_{39}N$) which I will continue to refer to using the manufacturers designation FC-71. In the case of N_2 dissipation causes the velocity profile to deviate substantially from the Blasius result for incompressible flows while the solution for FC-71 is indistinguishable from it within graphical accuracy, Kluwick (2000) [20]. Deviations from the classical boundary layer behaviour are caused not only by the smallness of the Eckert number but also by the unconventional gas dynamic properties of BZT fluids in the external inviscid

flow region. An example is provided by the interaction of a dense gas boundary layer with an oblique shock. Both diagrams in Fig.24 display distributions of the skin friction

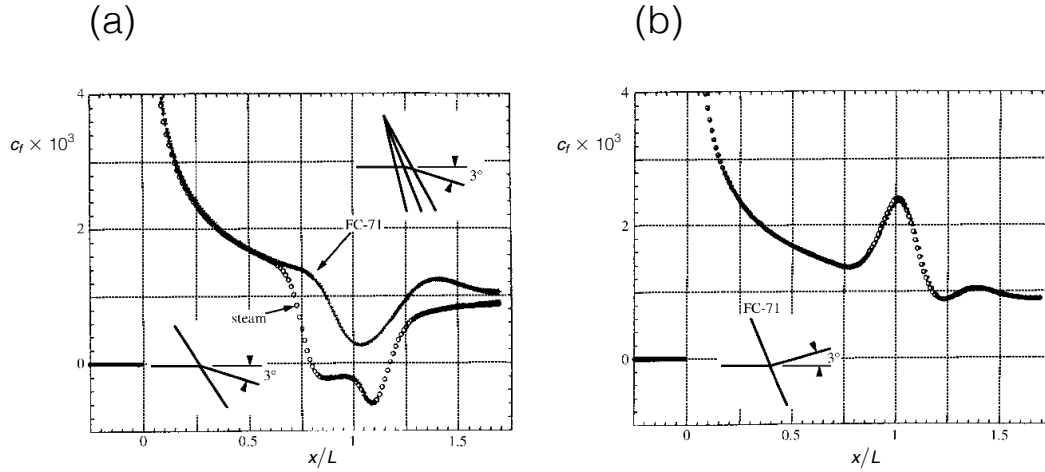


Figure 24. Flat plate boundary layer which interacts (a) with a weak compression wave and (b) with a weak rarefaction shock. $M_\infty = 2, T_\infty = 646.2K, P_\infty = 8.55atm$.

coefficient calculated by Cramer and Park (1999) [7]. In the case of steam the imposed deflection angle of 3 degrees leads to the formation of a compression shock which is strong enough to separate the boundary layer. In the case of FC-71 the same deflection angle leads to a smooth compression fan and the boundary layer remains attached. If the deflection angle is negative no shock discontinuity can form in a regular fluid such as steam but a rarefaction shock forms in the BZT fluid FC-71. Across this shock the fluid accelerates which in turn causes the wall shear to increase rather than to decrease.

Following this brief account of dense gas local interactions triggered by rapid pressure changes we turn to the last topic treated here: the effect of an adverse pressure gradient acting over a distance of $O(1)$ on the typical boundary layer length scale. A representative example is provided by linearly retarded flows. The streamwise velocity component in the external inviscid flow region then is of the form

$$u_e(x) = u_\infty \left(1 - \frac{x}{L}\right). \quad (31)$$

The incompressible version of this problem was investigated first by Howarth (1938) [15] and Hartree (1939) [14] who observed that the pressure increase associated with the imposed velocity decrease always leads to separation and that the numerical solution of the boundary layer equations cannot be continued beyond the point of zero wall shear. A related result holds for compressible flow past adiabatic walls if the fluid is a perfect gas or even a dense gas with low molecular complexity, Stewartson (1962) [26].

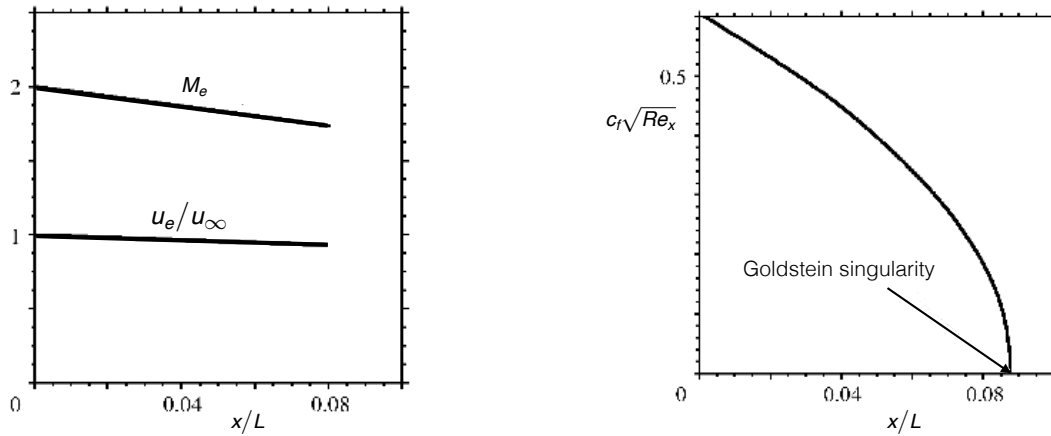


Figure 25. Linearly retarded flow for N_2 : $v_\infty = 5.009v_c$, $T_\infty = 1.001T_c$, $M_\infty = 2$, $R/c_{v_\infty} = 0.39$, $Ec = 0.72$.

As an example we consider Nitrogen with free stream conditions listed in Fig.25 where ρ_c and T_c denote the critical point density and temperature. Decreasing values of u_e lead to decreasing values of the local Mach number M_e at the boundary layer edge. The associated pressure increase causes the local friction coefficient c_f to decrease also and the skin friction distribution eventually tends to zero in an irregular manner known as Goldstein singularity, Goldstein (1948) [10].

Fig.26 shows what happens if the regular fluid N_2 is replaced by the BZT fluid FC-71. As before c_f drops initially but this tendency comes to a halt and c_f starts to rise despite the fact the pressure gradient is still unfavourable. A more detailed investigation of the flow suggests that this unconventional feature is closely related to the Mach number distribution at the boundary layer edge. In contrast to N_2 the isentropic compression of FC-71 causes M_e to increase rather than to decrease. Evaluation of the continuity equation outside the boundary layer then suggests that the displacement body felt by the external inviscid flow may shrink rather than expand in the streamwise direction. This is confirmed by numerical calculations. The associated momentum influx into the boundary layer is then able to overcome the onset of separation and causes c_f to rise sharply. Eventually, however, M_e drops which in turn quenches this effect so that the formation of a separation singularity is inevitable. Nevertheless the results plotted in Fig.26 clearly demonstrate the potential of dense gas flows to delay flow separation. If the free stream value v_∞ of the specific volume is slightly increased and approaches the critical value $v_{\infty_c} = 5.01v_c$ one obtains the limiting case shown in Fig.27: the wall shear vanishes in a single point but immediately recovers; at the point of zero wall shear the distribution of the displacement thickness δ exhibits a sharp corner. To resolve these physically unrealistic slope discontinuities we perform a

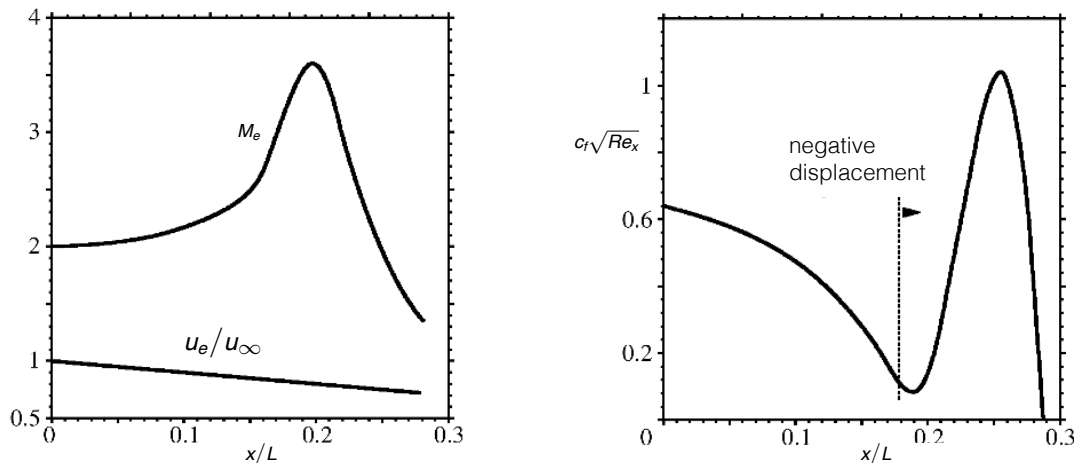


Figure 26. Linearly retarded flow for FC-71: $v_\infty = 5.009v_c$, $T_\infty = 1.001T_c$, $M_\infty = 2$, $R/c_{v_\infty} = 0.007$, $Ec = 0.015$.

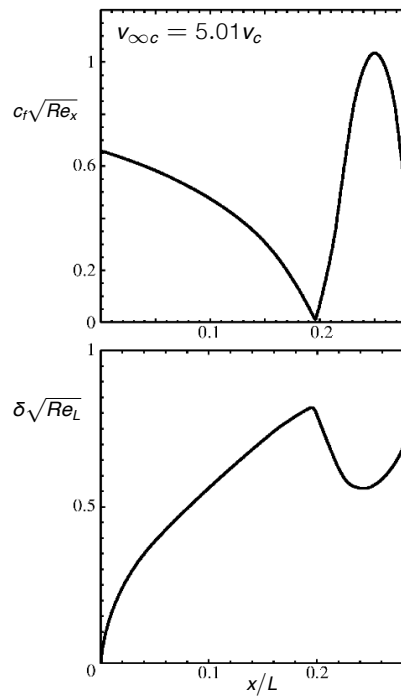


Figure 27. Linearly retarded flows for FC-71: $v_\infty = 5.01v_c$, $T_\infty = 1.001T_c$, $M_\infty = 2$, $R/c_{v_\infty} = 0.007$, $Ec = 0.015$.

local analysis based on the assumption that a further increase of v_∞ will result in the formation of a short separated flow region close to $x = x_s$ where classical boundary layer theory fails. Introducing stretched quantities X , A , and the parameter a which accounts for the difference between v_∞ and $v_{\infty c}$

$$a \propto Re^{\frac{2}{5}}(v_\infty - v_{\infty c}) \quad (32)$$

one finds that the scaled friction coefficient $A(X)$ satisfies the integro- differential equation

$$A^2(X) - X^2 + 2a = \lambda \int_{-\infty}^x \frac{A''(\xi)}{\sqrt{X - \xi}} d\xi \quad (33)$$

where λ is a positive constant, Kinell and Kluwick (2003) [16]. Solutions are shown in Fig.28. As expected A decreases with increasing values a and eventually the formation

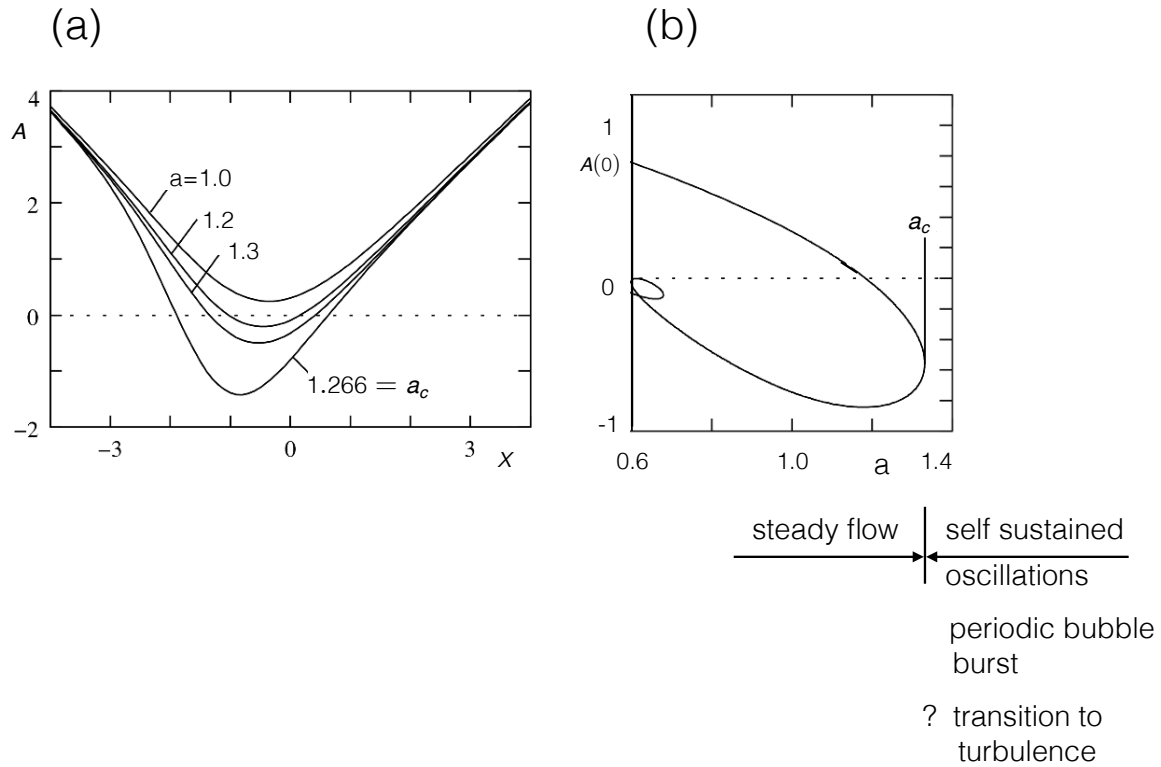


Figure 28. Marginally separated dense gas boundary layer: (a) wall-shear stress distributions for various values of a , (b) bifurcation diagram; transition from steady flow to self-sustained oscillations.

of a separated flow region where A is negative is observed, Fig.28a. Fig.28b displays the variation of $A(0)$ with a and it is seen that solutions of the interaction equation (33) form two branches: an upper branch where skin friction distributions are of the form depicted in Fig.28a and a lower branch which exhibits significantly larger recirculation

zones. Even more important, however, it is seen that steady solutions exist up to a critical value $a_c \doteq 1.266$ only. An extended analysis which includes both steady and unsteady effects indicates that the passage through a_c leads the onset of self-sustained oscillations associated with periodic bubble burst. These oscillations may possibly be interpreted as first signs of transition to turbulence but this represents another challenge for future research in the field of NICFD.

6. Conclusions

The present paper starts from the premise that negative Γ Fluids, so called Bethe-Zel'dovich-Thompson (BZT) fluids, exist and concentrates on non-classical aspects which arise in this context. To simplify the discussion inviscid weakly non-linear flows were considered first. Such an approach allows for significant analytical progress but still yields a complete qualitative picture of all possible new phenomena including rarefaction shocks, sonic shocks, double sonic shocks, split shocks, compression wave fans, the delay of shock formation by decreasing values of Γ , etc.. This is achieved by introducing the concept of the perturbation mass flux which applies to both steady and unsteady flows and simplifies the derivation of the three building blocks needed for the general understanding of these unconventional flow features: shock formation, wave evolution, shock propagation. Specific examples considered which might be of interest also in connection with experimental work to demonstrate existence of in particular rarefaction shocks are unidirectional acoustic waves, quasi one-dimensional nozzle flow and transonic two-dimensional flow past compression/expansion ramps. Besides providing results which are of importance for practical applications the treatment of these flows highlights another advantage of the present perturbation analysis, the emergence of non-dimensional similarity parameters which identify regimes of qualitatively different flow behaviour.

Following the discussion of inviscid flows in sections 2, 3 and 4 viscous effects are considered in section 5 which concentrates on laminar flows of boundary layer type. Specifically it is found that the Eckert number which characterises the importance of dissipation in the energy equation may be small not only for small values of the free stream Mach number but also for moderately large supersonic values. Other non-classical features arise from the unconventional fluid properties in the inviscid external inviscid flow region which may delay flow separation in cases of viscous inviscid interaction but also if an adverse pressure gradient acts over a distance of order one on the typical boundary layer length scale.

Acknowledgement

I would like to thank Dr. E. A. Cox for his invaluable assistance during the preparation of this manuscript. Without his help the manuscript could not have been published in its present form.

References

- [1] Becker R. (1922). Stoßwelle und Detonation. Zeitschrift für Physik 8: 321 - 362.
- [2] Bethe H.A. (1942). The theory of shock waves for an arbitrary equation of state. Report No. 545. Office of Scientific Research and Development.
- [3] Colonna P., Guardone A., Nannan N.R. (2007). Siloxanes: A new class of Bethe-Zel'dovich Thompson fluids. Phys. Fluids, 19(8): 086102-086113.
- [4] Cramer M.S., Kluwick, A. (1984). On the propagation of waves exhibiting both positive and negative nonlinearity. J. Fluid Mech. 142: 9 - 37.
- [5] Cramer M.S., Tarkenton G.M. (1992). Transonic flows of Bethe-Zel'dovich-Thompson fluids. J. Fluid Mech. 240: 197 - 228.
- [6] Cramer M.S., Fry R.N. (1993). Nozzle flows of dense gases. Phys. Fluids A 5: 1246 - 1259.
- [7] Cramer M.S., Park S. (1999). On the suppression of shock-induced separation in Bethe-Zel'dovich-Thompson fluids. J. Fluid Mech. 393: 1 - 21.
- [8] Duhem P. (1909). On the propagation of shock waves in fluids. Z. Phys. Chem. 69: 169 - 186.
- [9] Colonna P., Guardone A., Nannan N.R. (2007). Siloxanes: A new class of Bethe-Zel'dovich Thompson fluids. Phys. Fluids, 19(8): 086102-086114.
- [10] Goldstein S. (1948). On laminar boundary-layer flow near a position of separation. Q. J. Mech. Appl. Math. 1: 43 - 69.
- [11] Guardone A., Colonna P., Casati E., Rinaldi E. (2014). Non-classical gas dynamics of vapour mixtures. J. Fluid Mech. 741: 681 - 701.
- [12] Guardone A., Vimercati D., (2016) Exact solutions to non-classical steady nozzle flows of Bethe - Zel'dovich - Thompson fluids, J. Fluid Mech. 800: 278 - 306.
- [13] Hayes W.D. (1958). The Basic Theory of Gasdynamic Discontinuities, in H.W.Emmons, ed., Fundamentals of Gasdynamics, vol. 3, Princeton Series in High Speed Aerodynamics and Jet Propulsion, Princeton University Press, Princeton, N.J.
- [14] Hartree D. R. (1939). A solution of the laminar boundary-layer equations for retarded flow. Mem. Aero. Res. Coun., London, no 2426 (spec. vol. I.).
- [15] Howarth L. (1938). On the solution of the laminar boundary layer equations. Proc. R. Soc. Lond. A 164: 547 - 579.
- [16] Kinell M., Kluwick A. (2003). On a new form of marginal separation. PAMM 3: 358 - 359.
- [17] Kluwick A. (1991). Small-amplitude finite-rate waves in fluids having both positive and negative nonlinearity. In A. Kluwick, ed., Nonlinear Waves in Real Fluids, volume 315 of the International Centre for Mechanical Sciences, pp. 1 - 43. Springer Vienna.
- [18] Kluwick A. (1993). Transonic nozzle flow of dense gases. J. Fluid Mech. 247: 661 - 688.
- [19] Kluwick A., Scheichl St. (1996) Unsteady transonic nozzle flow of dense gases. J Fluid Mech. 310: 113 - 137.
- [20] Kluwick A. (2000). Marginally separated flows in dilute and dense gases. Phil. Trans. R. Soc. Lond. A 358: 3169 - 3192.
- [21] Kluwick A. (2001). Rarefaction Shocks. in: Handbook of Shock Waves, Vol 1, G. Ben-Dor, T. Elprin, O. Ingra (ed.); Academic Press, San Diego: 339-411.
- [22] Kluwick A., Cox E. A. (2016). Steady transonic dense gas flow past a two-dimensional compression/expansion ramp; Talk: 24th International Congress on Theoretical and Applied Mechanics (ICTAM 2016), Montréal, Canada; in: "Book of Papers", IUTAM, (2016), 1 - 2.
- [23] Lambrakis K.C., Thompson P. A. (1972). Existence of real fluids with a negative fundamental derivative Γ . The Physics of Fluids 15: 933 - 935.
- [24] Lax P.D. (1957). Hyperbolic systems of conservation laws II. Comm. Pure Appl. Math. 19: 537 - 566.
- [25] Oleinik O. (1959). Uniqueness and stability of the generalized solution of the Cauchy problem for a quasi-linear equation. Usp. Math. Nauk. 14: 165 - 170.
- [26] Stewartson K. (1962). The behaviour of a laminar compressible boundary layer near a point of

- zero skin friction. J. Fluid Mech. 12: 117 - 128.
- [27] Thompson, P.A. (1971). A Fundamental Derivative in Gas Dynamics. Physics of Fluids 14: 1843 - 1849.
- [28] Thompson P.A., Lambrakis K.C. (1973). Negative shock waves. J. Fluid Mech. 60 : 187 - 208.
- [29] Vimercati D.(2015) Exact solutions to non-classical, quasi-1D nozzle flows of Bethe-Zel'dovich-Thompson fluids. Tesi di laurea, Politecnico di Milano
- [30] Zel'dovich Ya.B. (1946). On the possibility of rarefaction shock waves. Zh. Eksp. Teor. Fiz. 4: 363 - 364.
- [31] Zieher F. (1993). Kompressible Grenzschichtströmungen bei Zuständen in der Nähe des kritischen Punktes. Masters Thesis, Vienna University of Technology, 1 - 44.